Self-assembly of Sidewall Functionalized Single-walled Carbon Nanotubes Investigated by Scanning Tunneling Microscopy

ARTICLE *in* THE JOURNAL OF PHYSICAL CHEMISTRY C · AUGUST 2008

Impact Factor: 4.77 · DOI: 10.1021/jp711658b

5 AUTHORS, INCLUDING:

Valery N Khabashesku
Rice University
106 PUBLICATIONS **3,603** CITATIONS
SEE PROFILE

Andrew R. Barron
Rice University
454 PUBLICATIONS **9,503** CITATIONS
SEE PROFILE

Kevin Kelly
Rice University
114 PUBLICATIONS **4,575** CITATIONS
SEE PROFILE

Self-assembly of Sidewall Functionalized Single-walled Carbon Nanotubes Investigated by Scanning Tunneling Microscopy

Jun Zhang,[†] Lei Zhang,[‡] Valery N. Khabashesku,[‡,§] Andrew R. Barron,[‡,§] and Kevin F. Kelly*[,†,§]

Department of Electrical and Computer Engineering and Department of Chemistry, Rice University, Houston, Texas 77005and Richard E. Smalley Institute for Nanoscale Science and Technology, Houston, Texas 77005

Received: December 11, 2007; Revised Manuscript Received: April 28, 2008

The thiol and thiophene sidewall functionalized single-walled carbon nanotubes have been investigated by scanning tunneling microscopy. By exploiting the well-established Au−S chemistry, the thiol- and thiophene-modified nanotubes were self-assembled and anchored on bare gold surfaces as well as inserted into hexanethiol self-assembled monolayers. The positions of functional groups on the nanotube sidewall are revealed during imaging. From these measurements we have determined the size and spatial distribution of the sulfur-functionalized sidechains along the nanotube sidewalls.

Introduction

Scanning tunneling microscopy has been widely used to investigate the physical and corresponding electrical properties of individual multiwalled and single-walled carbon nanotubes (SWNTs)[1–4] due to its extremely high resolution. The functionalization of SWNTs, in particular of the sidewalls, has recently become a key area of SWNT chemistry.[5,6] For the sidewall functionalization, successful nondestructive fluorination of SWNT sidewalls, which was demonstrated by Mickelson et al.,[7] has proven that it can significantly modify the intrinsic chemical and electronic properties of SWNTs, as compared with the end-limited modification.[8,9] Fluorinated nanotubes alone may provide building blocks of different functionality for molecular electronics;[10] however, additional nanotube chemistry would greatly enhance the viability of nanotubes in such applications. As compared to infrared (IR), Raman, and thermogravimetric analysis (TGA), probe microscopies including atomic force microscopy (AFM) and scanning tunneling microscopy (STM) have been scarcely applied to study the functionalization of carbon nanotubes,[11,12] probably due to the difficulty of imaging. We do this in our study because the difficulty is worth the resolution and because scanning probes have proven especially beneficial when monitoring the intricacies of self-assembly.[13]

Fluorinated nanotubes are the essential precursor in many chemical reactions for further modification by substitution of other organic functional groups, such as N-alkylidene amino groups.[6,14,15] Following this method, we induced thiol- and thiophene-terminated alkane chains to covalently bond to the nanotube sidewall,[16] as shown in Scheme 1a, for subsequent self-assembly onto bare gold substrates based upon the well-established Au−S chemistry. In addition, the functionalized SWNTs also lend themselves to insertion in preformed alkanethiolate self-assembled monolayers (SAM) on gold substrates where the chemically reactive functional groups will naturally insert into the domain boundaries and defect sites of the SAM,[13,17] as shown in Scheme 1b.

SCHEME 1: (a) Illustration of functionalized SWNTs, where R represents the thiol or thiophene functional group. (b) Schematic of functionalized SWNT, which is inserted into hexanethiol SAMs and attaches to the gold surface

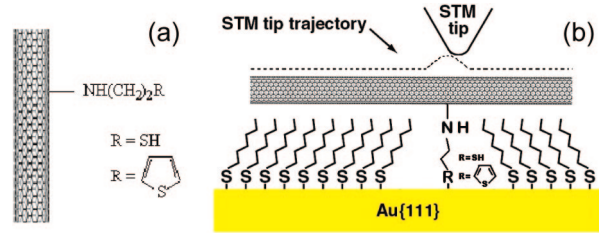

Experimental Section

For these experiments, the starting material consisted of HiPCO SWNTs produced by Carbon Nanotechnology Laboratory at Rice University that were purified to remove iron and other impurities[18] and subsequently fluorinated to achieve a C/F ratio of approximately 12:5, by direct fluorination at 150 °C as previously described.[15] The fluorotubes were then reacted with the appropriate amine in the presence of a base catalyst to create the final functionalized SWNTs that are shown in the Scheme 1a. The IR spectra of thiol- and thiophene-functionalized carbon nanotubes yield signatures associated with the substituents that confirm successful attachment.[16] The thiol- and thiophene-functionalized product can be dissolved in various organic solvents such as dimethyl formamide (DMF), isopropanol (IPA), and ethanol. The powder from both the thiol and thiophene functionalized nanotubes was placed in a moderate quantity of DMF solvent and then sonicated for 10−15 min.[19] To perform the comparison experiments, pristine SWNT solutions were suspended at a similar concentration in DMF solvent by sonication. Spin-coating is the common deposition method for dispersing carbon nanotubes onto a surface. It is expected that the reactive terminal groups of thiol- or thiophene-functionalized SWNTs will allow facile and even deposition of tubes to the Au surface by immersing substrates nanotube solutions.

The alkanethiol family of molecules including butanethiol, hexanethiol, octanethiol and decanethiol were used to prepare

* Corresponding author e-mail: kkelly@rice.edu; phone: 713-348-3565; fax: 713-348-5686.
† Department of Electrical and Computer Engineering, Rice University.
‡ Department of Chemistry, Rice University.
§ Richard E. Smalley Institute for Nanoscale Science and Technology.

10.1021/jp711658b CCC: $40.75
Published on Web 07/23/2008

alkanethiolate monolayers suitable for insertion experiments[20] via assembly onto hydrogen flame-annealed Au(111) on mica.[21] Monolayer formation on the Au(111) on mica was performed by immersing the substrate into 1 mM alkanethiolate in ethanol for 1 h, although some defect sites and vacancy islands (etch pits) remain in the molecular monolayer.[13,22,23] After removal, the samples went through repeated ethanol rinses and were then dried with nitrogen. Further, the quality of the SAMs was confirmed by imaging with the STM prior to exposure to the nanotube solutions by imaging domains, domain boundaries, and various defects, as well as clear resolution of the molecular lattice. The tunneling microscopy measurements reported here were performed by using a home-built, inchworm-based[24] STM[25] under ambient conditions. To reduce the tip−nanotube interactions[26] and tip-induced image artifacts such as multiple-tip effects, C_{60}-adsorbed tips were employed.[27,28] The images were obtained in the constant-current operating mode.

Results

To understand and explore the self-assembly of thiol- and thiophene-functionalized SWNTs, four comparison experiments were performed for both types of carbon nanotube. Initially, we immersed Au(111) on mica substrates into a solution of pristine SWNTs for 30 min. After removing the sample from solution, it was repeatedly rinsed with ethanol and then dried in a stream of nitrogen gas. Upon scanning the sample in STM, we did not observe any nanotubes on the substrate. They were presumably removed during the rinsing process since they lacked a strong enough bonding interaction with the gold. Upon repeating the above procedure, but instead replacing the pristine tubes with the other variation of sidewall functionalized nanotubes, the STM images revealed many nanotubes decorating the gold surface. An example from a thiophene functionalized nanotube sample is shown in Figure 1a. Next, we repeated a similar procedure, but substitute alkanethiol SAMs on gold in place of the bare gold substrate, and then immersed these samples into the pristine SWNTs solution for 30 min. After rinsing with ethanol and drying, these samples were imaged with the STM. The hexanethiol SAMs appeared intact and crystalline; nevertheless, no nanotubes were found on the surface. Lastly, the alkanethiolate-coated gold substrates were immersed in the functionalized SWNT solutions. When these samples were scanned, we observed that the functionalized SWNTs were inserted into the preformed alkanethiol SAMs and became strongly bound to the underlying gold surface. Figure 1b shows an example of the thiophene functionalized nanotubes inserted into a 1-h hexanethiol monolayer. Comparing the results of these experiments, we concluded that the thiol and thiophene sidewall functional groups work well as anchors for binding tubes to bare gold surfaces or inserting them into alkanethiol matrices (illustrated in Scheme 1b), and that the Au−thiol and Au−thiophene bonds are fairly robust. It should be noted that this is the first instance where a thiophene-terminated linker has been employed for insertion and bonding in preformed SAMs. Self-assembly via thiophene termination may also offer potential advantages over thiols for use in molecular electronics, because the Au−thiol bonding is known to maintain a small barrier to charge transfer.[29]

Further evaluation of Figure 1, panels a and b, reveals an additional difference between the functionalized SWNTs placed directly on a bare gold surface and inserted into the preformed SAMs. There is a significant perturbation of the carbon nanotubes during the STM imaging with them on a bare gold surface. In this case, where the STM tip is sweeping horizontally

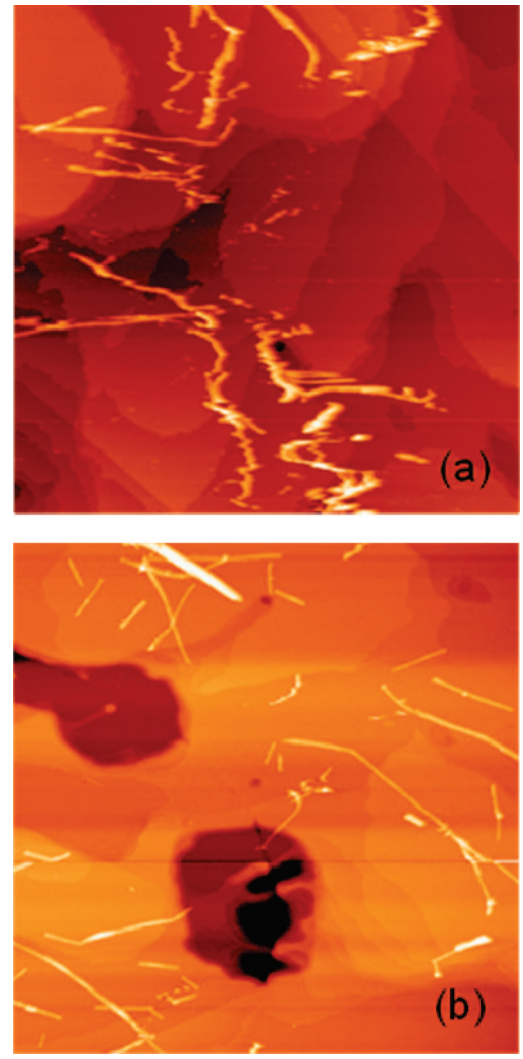

Figure 1. (a) STM image (600 × 600 nm, $V_b = -0.8$ V, $I_t = 5$ pA) of thiophene-functionalized SWNTs that are placed on a bare gold surface. (b) STM image (600 × 600 nm, $V_b = -0.8$ V, $I_t = 25$ pA) of thiophene-functionalized SWNTs that are inserted into hexanethiol SAMs.

across the images, the tubes, which are near perpendicular to the fast scan direction, were likely being moved or cut by the STM tip during scanning. It was difficult to achieve stable images of functionalized tubes using this method of deposition. The possible reasons for the perturbation by the STM tip are three-fold. First, the functional molecular side chain has a fixed length (>1 nm). When the thiophene head is attached to the Au, the whole sidewall molecule will probably remain upright on the bare Au surface. Even though the molecules may increase the binding of the nanotubes to the Au surface, the tubes may still be moved a certain distance given the slack provided by the length of the molecule and due to the electrostatic interaction previously observed between the STM tip and nanotubes.[30] However, this distance would be constrained by the small length of the sidewall molecules. Second, although the Au−S bond is very strong in desorption, for example, powerful enough to hold the tubes on the Au surface, the diffusion energy needed when moving alkanethiols and other sulfur-terminated molecules on the Au surface is relatively small when present in low coverages. Poirier et al.[31] illustrated this principle when they studied the liquid phase of alkanethiolate SAMs in low coverage on gold by STM. One might expect the mobility of the sulfur-terminated molecules is relatively high on the Au surface in the case of

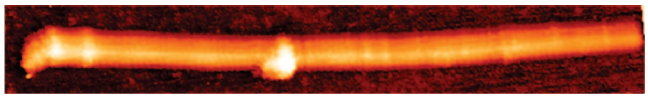

Figure 2. A high-resolution STM image (120 × 17 nm, $V_b = -0.8$ V, $I_t = 30$ pA) of a thiophene-functionalized SWNT inserted into hexanethiol SAMs, where two types of defect are observed.

the bare gold given the sparsity of the sidewall anchors. From this perspective, the movement of sidewall functionalized tubes on Au is not unreasonable. Third, the sulfur-terminated molecules not bound to the gold due to their location on the upper side of the nanotube could be "grabbing at" and temporarily bonding to some part of the tip via a Pt−S bond. Such a bond has been shown to be nearly equivalent to its Au−S counterpart, 45−75 kcal mol^{-1} depending on the sulfur species.[32] Correspondingly, we observed an improvement in the STM image quality as shown in Figure 1b when the functional group is inserted into the SAMs, because both of the first two possibilities for the Au−S movement were eliminated. The sidewall functional groups are forced to stand up by the close-packed SAM molecular matrix. In addition, the close-packed sulfur atoms from alkanethiolate molecules on the Au surface blocked the diffusion of thiol or thiophene terminations. The third reason for nanotube movement during scanning has been limited and weakened because a greater majority of the thiophene groups are inserted compared to the few that are exposed and have an opportunity to chemically interact with the tip. Therefore, the STM can stably and clearly identify the individual nanotubes, as well as reveal the defect structures along the tubes. Meanwhile, the atomic images of the underlying hexanethiol SAM demonstrate that the SAMs were not adversely affected by the nanotube solution during the insertion process. Although a more detailed investigation has yet to be performed, it was preliminarily found that the length of the SAM molecules also plays a role. After comparing butanethiol, hexanethiol, octanethiol, and decanethiol as candidate SAM molecules in the insertion experiments, hexanethiol SAMs yielded the best insertion and imaging result, probably due to their comparable length to the functional groups along the nanotube sidewalls.

A more detailed investigation of the thiophene-functionalized SWNTs in hexanethiol SAMs was performed, and the results were compared with the pristine SWNT starting material. We observed a number of defects along the length of the thiophene tubes, which reflect both structural changes of the sp^2 lattice of the tube sidewall as well as additionally reflecting a change in the local electronic properties. Classifying by size, we find two sizes of defects associated with the sidewall chemistry. An example of this can be clearly observed for the nanotube displayed in Figure 2, where there are three large defects and many small defects present along its length. Figure 3 shows a high resolution image of the area around one large defect on the same tube, although individual carbon atoms were not clearly resolved.[33] Its corresponding 3-D view and the cross-section are also shown. The defect structures can be clearly identified; there is one large defect and four small defects observed in both the STM image and the cross-section view. As with all probe microscopies, the cross-sectional height measurement better reflects the nature of objects more accurately than the width observed in the 2-D image since this contains artifacts due to convolution with the tip structure. The relative height of the large defect to the bare areas of nanotube is ~1.5 nm. When taking the cross-section of small defects on the tubes, seen in Figure 4, it is found that the relative heights are only about 0.5 nm.

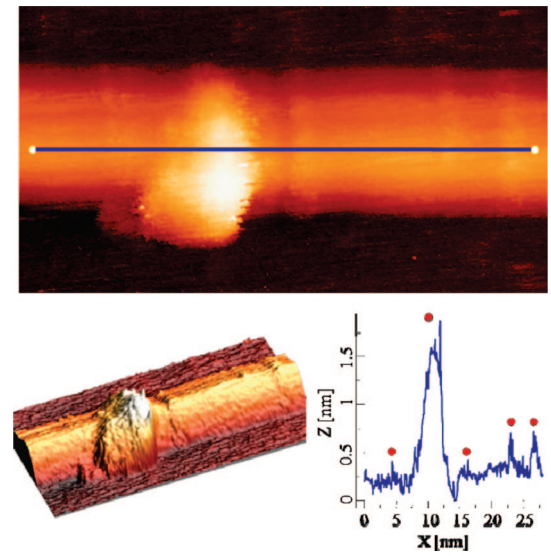

Figure 3. An enlarged STM image (30 × 15 nm, $V_b = -0.8$ V, $I_t = 30$ pA) and the corresponding 3-D view of the area around one large defect on the thiophene nanotube. The lower right panel is the cross-section.

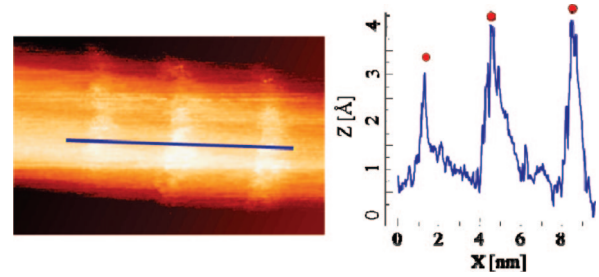

Figure 4. STM image (10 × 8 nm, $V_b = -0.3$ V, $I_t = 30$ pA) and the cross-section of small defects on a thiophene functionalized SWNT.

SCHEME 2: Illustration of possible reasons for the difference between small and large defects. The left schematic shows a small defect, and the right shows a large defect.

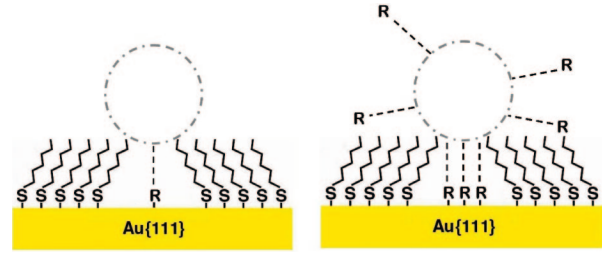

Discussion

We attribute the defects seen in the STM images to the presence of the thiophene functional groups that are covalently bound to the nanotube sidewall. First, both experiments and theoretical studies reveal that covalent functionalization has a strong effect on the electronic properties of the nanotube.[11,34] The defects we observed would likely modulate the electronic states along the nanotube induced by the presence of the attached functional groups and are prominently imaged by the STM. Second, the bumps along the tubes in the STM images may also imply that the tunneling conductance between the tip and substrate is different at the functional defect sites. As illustrated in Scheme 1b, the functional groups may provide conducting channels between the tube and Au surface, whereas other parts

TABLE 1: Defect Spatial Distribution of Thiophene-functionalized SWNTs

defect type	number of defects measured	total length of SWNTs measured (nm)	spatial distance between defects (nm)	defect density (per nm)
large	159	7860	49.4 ± 29.5	0.02
small	388	5380	13.9 ± 10.6	0.07

of the nanotube remain relatively electronically isolated from the metal surface by the underlying alkanethiol SAM molecules.

A few possible reasons for the distinction of the two types of defects are summarized in Scheme 2. Because the small defects might have only one or very few functional groups attached at the same functional site of the nanotube sidewall, the large defects could indicate more functional groups attached, or the large defects themselves might point out dangling side groups not bound to the Au surface. It is also possible that the graphite lattice of the SWNTs has some chemically induced defects created during the chemical process of functionalization that can cause electronic property changes resulting in the large defects. Of course, the result may be a result from any combination of the above-mentioned possibilities. After analyzing a large quantity of thiophene-functionalized SWNTs by taking cross-section in the STM images, the thiophene-functionalized SWNTs show a fairly even distribution of defects. A summary of the defect spatial distribution is shown in Table 1. In total, the average spatial distance between each of the two defects, including both large and small defects, is about 11 nm.

The thiol-functionalized SWNTs have been similarly investigated. However, in Figure 5, the defects in the STM image of thiol-functionalized SWNTs inserted into SAMs are seen as much bigger than the ones found on the thiophene tubes, by analyzing the cross-sections. It is quite probably that the thiol groups have relatively dissimilar electronic properties and possibly different chemical bonding structures as well. The difference between the defect structures of the thiol- and thiophene-functionalized SWNTs, observed by STM, corresponds very well to our previous AFM results.[16] By reacting the exposed thiol or thiophene terminations with gold nanoparticles (~5 nm) and using them as a chemical marker[35] for the reactive sites, we have previously studied functionalized SWNTs by AFM.[16] Our AFM results revealed that the Au nanoparticles were attached in unevenly spaced agglomerations along the length of the thiol functionalized SWNTs. In contrast, the thiophene tubes showed large regions of continuous Au-functionalized regions. Combined with TGA and Raman analysis, we have concluded that with the similar levels of functionalization, the thiol functional groups are likely to combine together and bind to one Au nanoparticle, whereas the thiophene groups appear more evenly distributed along the nanotubes and have as few as one Au nanoparticle per molecule. This means that, during our insertion experiment, several thiol groups will bundle together, resulting in the appearance of a larger defect site in the STM image.

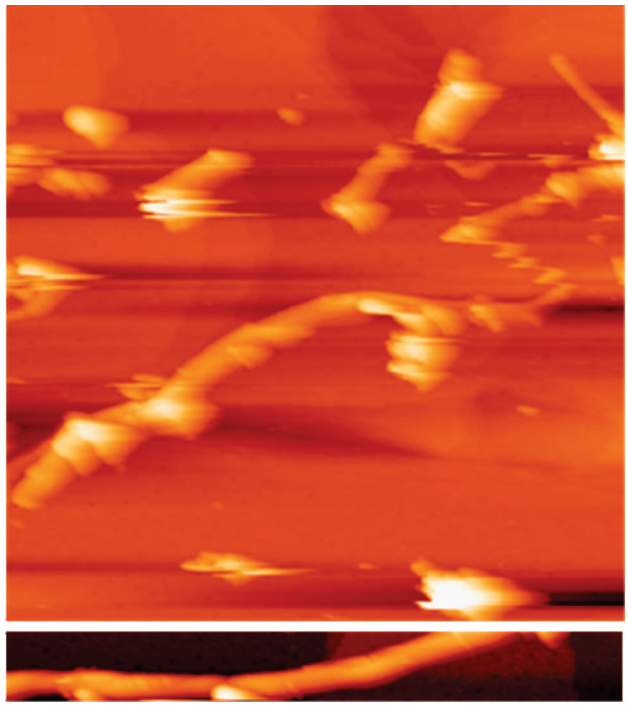

Figure 5. (Top) STM image (400 × 400 nm, $V_b = -0.5$ V, $I_t = 3$ pA) of thiol-functionalized SWNTs inserted into hexanethiol SAMs, where the big defects on the thiol nanotubes are observed. (Bottom) A high-resolution STM image (360 × 40 nm, $V_b = -0.6$ V, $I_t = 4$ pA) of a thiol-functionalized SWNT inserted into hexanethiol SAMs.

Self-assembly and insertion of functionalized SWNTs has many potential applications since self-assembly has proven itself a powerful technique for chemically patterning surfaces and building electronic devices at the nanometer level. Our experiments have demonstrated that functionalized SWNTs could be patterned in a similar manner to previous techniques, such as microcontact printing,[36] dip-pen lithography,[37,38] etc. Along these lines, it may be possible for SWNTs to be patterned by insertion with functionalized alkanethiolate SAMs for future transistor applications. Dai et al.[39] have already performed SWNT doping experiments where nanotube PN junctions and transistors were created by combining the bulk lithography with chemical adsorption of amine groups to the SWNTs. Although successful, this method limited the resolution of doping to hundreds of nanometers, due to the use of bulk lithographic techniques. However, the chemical doping method we propose based on the results of these investigations could result in truly molecular-patterned nanotube devices at single nanometer scale.

Conclusions

We have investigated self-assembly and insertion of the thiol- and thiophene-functionalized SWNTs by utilizing gold−sulfur chemical bonds. The individual functionalized SWNTs and their functional structures were clearly observed in our STM images when they were inserted into the preformed hexanethiol SAMs on a gold surface. The sizes and the spatial distribution of the defects were measured by taking the cross-section on the STM images. In the future, we hope to perform scanning tunneling spectroscopy (STS) at the bonding sites on the SWNT sidewall to further probe the electronic characteristic of chemical functionalization.

Acknowledgment. The authors gratefully acknowledge support from the Welch Foundation, the Air Force Office of Scientific Research (W911NF-04-01-0203), the Army Research Office (F49620-03-1-0379), and Carbon Nanotechnologies, Inc.

Note Added after ASAP Publication. This article posted ASAP on July 23, 2008. The title has been revised. The correct version posted on August 7, 2008.

References and Notes

(1) Ge, M.; Sattler, K. *Science* **1993**, *260*, 515.

(2) Ge, M.; Sattler, K. *Appl. Phys. Lett.* **1994**, *65*, 2284.

(3) Wilder, J. W. G.; Venema, L. C.; Rinzler, A. G.; Smalley, R. E.; Dekker, C. *Nature* **1998**, *391*, 59.

(4) Odom, T. W.; Huang, J.; Kim, P.; Lieber, C. M. *Nature* **1998**, *391*, 62.

(5) Sun, Y.; Fu, K.; Lin, Y.; Huang, W. *Acc. Chem. Res.* **2002**, *35*, 1096.

(6) Khabashesku, V. N.; Billups, W. E.; Margrave, J. L. *Acc. Chem. Res.* **2002**, *35*, 1087.

(7) Mickelson, E. T.; Huffman, C. B.; Rinzler, A. G.; Smalley, R. E.; Hauge, R. H.; Margrave, J. L. *Chem. Phys. Lett.* **1998**, *296*, 188.

(8) Chen, J.; Hamon, M. A.; Hu, H.; Chen, Y.; Rao, A. M.; Eklund, P. C.; Haddon, R. C. *Science* **1998**, (282), 95.

(9) Liu, J.; Rinzler, A. G.; Dai, H.; Hafner, J. H.; Bradley, R. K.; Boul, P. J.; Lu, A.; Iverson, T.; Shelimov, K.; Huffman, C. B.; Rodriguez-Macias, F.; Shon, Y.; Lee, T. R.; Colbert, D. T.; Smalley, R. E. *Science* **1998**, *280*, 1253.

(10) Seifert, G.; Kohler, T.; Frauenheim, T. *Appl. Phys. Lett.* **2000**, *77*, 1313.

(11) Kelly, K. F.; Chiang, I. W.; Mickelson, E. T.; Hauge, R. H.; Margrave, J. L.; Wang, X.; Scuseria, G. E.; Radloff, C.; Halas, N. J. *Chem. Phys. Lett.* **1999**, *445*, 313.

(12) Bonifazi, D.; Nacci, C.; Marega, R.; Campidelli, S.; Ceballos, G.; Modesti, S.; Meneghetti, M.; Prato, M. *Nano Lett.* **2006**, *6*, 1408.

(13) Smith, R. K.; Lewis, P. A.; Weiss, P. S. *Prog. Surf. Sci.* **2004**, *75*, 1.

(14) Stevens, J. L.; Huang, A. Y.; Peng, H.; Chiang, I. W.; Khabashesku, V. N.; Margrave, J. L. *Nano Lett.* **2003**, *3*, 331.

(15) Zhang, L.; Kiny, V. U.; Peng, H.; Zhu, J.; Lobo, R. F. M.; Margrave, J. L.; Khabashesku, V. N. *Chem. Mater.* **2004**, *16*, 2055.

(16) Zhang, L.; Zhang, J.; Khabashesku, V. N.; Kelly, K. F.; Barron, A. R. *Chem. Com.* **2005**, *43*, 5429.

(17) Bumm, L. A.; Arnold, J. J.; Cygan, M. T.; Dunbar, T. D.; Burgin, T. P.; Jones, L. I.; Allara, D. L.; Tour, J. M.; Weiss, P. S. *Science* **1996**, *271*, 1705.

(18) Chiang, I. W.; Brinson, B. E.; Huang, A. Y.; Willis, P. A.; Bronikowski, M. J.; Margrave, J. L.; Smalley, R. E.; Hauge, R. H. *J. Phys. Chem. B* **2001**, *105*, 8297.

(19) A long sonication time should be avoided, otherwise the tubes have been found to breakdown to shorter pieces that were not imaged stably enough for these studies.

(20) Purchased from Sigma-Aldrich Co., St. Louis, Missouri.

(21) Purchased from Agilent Technologies (Molecular Imaging Co.), Tempe, Arizona.

(22) Poirier, G. E.; Pylant, E. D. *Science* **1996**, *272*, 1145.

(23) Poirier, G. E. *Langmuir* **1997**, *13*, 2019.

(24) Purchased from EXFO Burleigh, Plano, Texas.

(25) Operated by a RHK SPM100 controller and software, RHK Technology Inc., Troy, Michigan.

(26) Zha, F.-X.; Czerw, R.; Carroll, D. L.; Kohler-Redlich, P.; Wei, B.-Q.; Loiseau, A.; Roth, S. *Phys. Rev. B* **2000**, *61* (7), 4884.

(27) Resh, J.; Sarkar, D.; Kulik, J.; Brueck, J.; Ignatiev, A.; Halas, N. J. *Surf. Sci.* **1994**, *316*, L1061.

(28) Kelly, K. F.; Sarkar, D.; Hale, G. D.; Oldenburg, S. J.; Halas, N. J. *Science* **1996**, *273*, 1371.

(29) Zhou, C.; Deshpande, M. R.; Reed, M. A.; II, L. J.; Tour, J. M. *Appl. Phys. Lett.* **1997**, *71* (5), 611.

(30) Curran, S.; Carroll, D. L.; Ajayan, P. M.; Redlich, P.; Roth, S.; Ruhle, M.; Blau, W. *Adv. Mater.* **1998**, *10* (4), 311.

(31) Poirier, G. E.; Fitts, W. P.; White, J. M. *Langmuir* **2001**, *17*, 1176.

(32) Rodriguez, J. A.; Hrbek, J.; Kuhn, M.; Jirsak, T.; Chaturvedi, S.; Maiti, A. *J. Cem. Phys.* **2000**, *113*, 11284.

(33) Only near-atomic resolution has been achieved, because the small tunneling gap, which is necessary for atomic resolution of SWNTs, cannot be reached due to the intrinsic insulating properties of underlying alkanethiolate SAMs and their imaging requirement of a large tunneling gap.

(34) Park, H.; Zhao, J.; Lu, J. P. *Nanotechnology* **2005**, *16*, 635.

(35) Coleman, K. S.; Bailey, S. R.; Fogden, S.; Green, M. L. H. *J. Am. Chem. Soc.* **2003**, *125*, 8722.

(36) Xia, Y.; Whitesides, G. M. *Angew. Chem., Int. Ed.* **1998**, *37*, 551.

(37) Piner, R. D.; Zhu, J.; Xu, F.; Hong, S.; Mirkin, C. A. *Science* **1999**, *283*, 661.

(38) Hong, S.; Zhu, J.; Mirkin, C. A. *Science* **1999**, *286*, 523.

(39) Kong, J.; Dai, H. *J. Phys. Chem. B* **2001**, *105*, 2890.

JP711658B